ELSEVIER

PII: S0032-3861(96)00662-3

Polymer Vol. 38 No. 7, pp. 1631–1637, 1997

0032-3861/97/$17.00+0.00

Preparation of asymmetric porous membranes of poly(vinyl chloride)

Tohru Kawai and Young Moo Lee*
Department of Industrial Chemistry, College of Engineering, Hanyang University, Seoul, 133-791, Korea

and Sumito Yamada
Department of Polymer, Faculty of Engineering, Tokyo Institute of Technology, Tokyo, Japan
(Received 8 March 1996; revised 20 March 1996)

The formation of the poly(vinyl chloride) (PVC) asymmetric porous membranes was investigated as a function of the evaporation time after casting PVC solutions in the mixture of tetrahydrofuran (THF) and water and in dimethylformamide (DMF), respectively. First, the phase diagram of the three components system, including the critical point, was obtained. In the case of the PVC/THF/water system, it was found that the particles composing the polymer-lean phases grew by the coarsening in the spinodal decomposition, resulting in the continuous structure and rather homogeneous, non-circular pores were formed on casting from a 6.8% polymer solution. From a 1.8% polymer solution, the particles composed of the polymer-rich phase came out, but they could not make the continuous membrane. However, the nucleation and growth mechanism may hold in this case. After immersing the membrane into water, the membranes became asymmetric after drying. In the case where the PVC solution in DMF was cast, the phase separation occurred cooperatively by the evaporation of DMF and the absorption of water by DMF at high relative humidity conditions. The observation of the PVC solution in the mixture of THF and water under a microscope showed that the particles formed from the polymer-lean phase grew in the matrix of the polymer-rich phase, resulting in the pores surrounded by a continuous, compact structure with a similar morphology to the PVC/THF/water system, which is considered to come from the polymer-rich phase. The flux of methanol through the membrane and accordingly, the mean pore radius showed a maximum with the evaporation time, at the cloud point. The decrease in the mean pore radius after the cloud point seems to be due to the shrinkage of the membrane during the precipitation and the drying.

(Keywords: PVC membrane; membrane formation; phase diagram)

INTRODUCTION

Since the pioneering work done by Loeb and Sourirajan[1] on integrally skinned asymmetric cellulose acetate membranes for reverse osmosis, the technologies on various types of the asymmetric and composite membranes, including hollow fibres, have been extensively developed[2]. The basic mechanism of the formation of such membranes has also been studied by many investigators and nearly established[2]. It is generally believed that the microporous substructure of asymmetric membranes originates from nucleation and growth of the polymer-lean phase in the polymer/solvent/nonsolvent systems[3–6]. The spinodal decomposition, which results in a regular, highly interconnected structure, has also been proposed for skin layer[3,6,7] as well as structural formation[8] of asymmetric membranes.

Most commonly, membrane structures have been investigated by microscopic techniques to gain some information about the possible phase separation mode responsible for the structural formation. However, a direct proof for either nucleation and growth or spinodal decomposition by microscopic analysis is difficult. A direct evidence for either mechanisms can only be established by the determination of the continuous compositional changes during the phase separation processes. Among huge numbers of publications on asymmetric membranes, only very few papers have dealt with this point[9–12].

On these grounds, in this paper, the process of the formation of asymmetric porous membranes of poly(vinyl chloride) (PVC), one of the most widely used polymers, has been pursued with time by evaporating the solvents, tetrahydrofran (THF) or dimethylformamide (DMF) from the PVC solutions or the three components system involving water as a non-solvent. This work is a rather fundamental study to gain basic information on the pore formation in the asymmetric membranes in general, but also may afford information on the application of PVC porous membranes to ultrafiltration.

EXPERIMENTAL

Materials

PVC used is a commercial product of Kishida Chem.

* To whom correspondence should be addressed

Co. The weight average molecular weight, $\bar{M}_w$ was 7.32×10^5, which was calculated from intrinsic viscosity, $[\eta]$, measured in THF at 30°C, from the equation[13]

$$[\eta] = 6.38 \times 10^{-2} M_w^{-0.65} \quad (1)$$

All the solvents used were of purity more than 99.9%.

Determination of phase diagram

Cloud points of the PVC/THF/water system were measured at 20°C visually by dropping water into the various compositions of PVC solutions in THF. The critical point was determined as follows. Keeping the PVC/THF ratio constant, and changing the water content in the system, the ratio of the two phases separated was measured for several instances. By plotting the phase ratio obtained against the water content, the composition, where the phase ratio is unity was obtained. Next, by the similar experiments changing the compositions of PVC and THF, several compositions of the three components system, where the phase ratio is unity, could be plotted in the phase diagram. The interest point of the curve connecting these points with the cloud point curve obtained previously is the critical point.

Observation of phase separation and measurement of phase equilibrium

In the case of the PVC/THF/water system, the solution of PVC (0.9 wt%), THF (83.9%) and water (9.2%) was dropped on the slide glass of an optical microscope and the phase separation, occurred by the evaporation of THF, was observed under the microscope at 20°C. Phase equilibrium of this system was also studied by keeping the solution in a closed glass tube at 20°C until reaching equilibrium, and by analysing the compositions of the polymer-rich and polymer-lean phases, respectively, by gas chromatography (by Model GC-7AG of Shimazu Co.). Polymer weight in the two phases was measured after evaporation.

Preparation of the membrane

Various concentrations of PVC solutions in THF/water mixtures and in DMF were prepared. Sometimes, methanol and calcium chloride ($CaCl_2$) were added to the solution. The PVC solution was developed onto a glass plate at 33.5°C under the relative humidity (RH) of 65% with a thickness of 300 μm or 500 μm, by using an automatic applicator from Camag Co. In the case of the PVC/THF/water system, the porous membrane was prepared by evaporating THF at 20°C for 1 h, washed repeatedly with water and methanol and dried under vacuum. In the case of the PVC solution in DMF, the porous membrane was obtained by evaporating DMF for 10 s to 20 min, followed by immersing into water at 25°C for 24 h. Microphase separation occurred by the sorption of water in air by DMF and the evaporation of DMF. After immersing into water, the membrane was washed with water, immersed in methanol for 24 h, dried at room temperature for a day, and dried under vacuum.

Measurement of sorption of water by DMF

The transient change in the water content in 5.0 cm^3 DMF in a petri dish with the diameter of 7 cm was measured at 33.5°C under RH of 65%, by using the Karl Fischer titrator.

Measurement of the change in the weight of the PVC solution with time

The change in the weight of a 11.2% PVC solution in DMF in a flask was measured at 32°C under the RH of 65%.

Measurement of temperature rise during the formation of the membrane

The temperature of the membrane cast from a 9.52% PVC solution in DMF was measured at 33.5°C under RH of 15, 51, 65 and 93%, respectively, by a usual thermal sensor inserted in the solution, as a function of time. RH was adjusted by using saturated solutions of $LiCl \cdot H_2O$, $Mg(NO_3)_2 \cdot 6H_2O$, $NaNO_2$, and KNO_3 for 15, 51, 65 and 93% respectively, as the substrate in the desiccator.

Characterization of the membrane

The number average radius, $\bar{r}_e$, of the pores on the surface of the membrane was determined from many transmission electron micrographs (TEM) of the surfaces. The electron microscope used was model JSM-U3 of JEOL in Japan. The scanning electron microscope (SEM) HU-11C Hitachi Co. was used to see the structures of the top and bottom surfaces and the cross-section of the membrane.

Porosity, P_r (%), of the total membrane was determined from the apparent density, ρ_f, calculated from the weight of the membrane with known area, and the thickness measured by using the equation:

$$P_r = (1 - \rho_f/\rho_p) \times 100 \quad (2)$$

where ρ_p is the density of the polymer at the measuring temperature (i.e., 25°C).

Measurement of flux of methanol

The flux, J_f, of methanol in units of $cm^3\,cm^{-2}\,s^{-1}\,mmHg^{-1}$ through the membrane was measured by apparatus described elsewhere[14]. The mean pore radius, $\bar{r}_f$, was calculated by the Hagen–Poiseuille equation:

$$\bar{r}_f = K\left(\frac{J_f d}{\Delta P P_r}\right)^{1/2} \quad (3)$$

where d is the thickness of the membrane (i.e., the average length of capillaries), and ΔP is the pressure

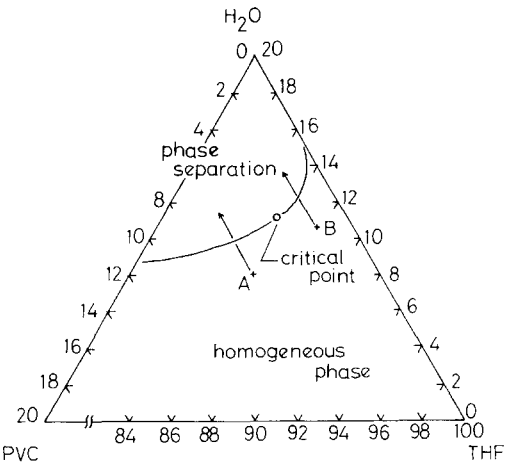

Figure 1 Phase diagram of the PVC/THF/water system at 20°C

difference across the membrane. K can be calculated either by using the membrane with known $\bar{r}_f$ or as $(8\eta)^{1/2}$, where η is the viscosity of the penetrant[15]. In this case, the latter method was adapted.

RESULTS AND DISCUSSION

PVC/THF/water system

Figure 1 shows the phase diagram of the PVC/THF/water system obtained at 20°C. Starting from the point A in the figure, i.e. the composition of PVC/THF/water is 6.8/83.9/9.2 wt%, the phase separation was observed under a microscope on a slide glass. Phase separation occurred by the evaporation of THF, corresponding to going up along the line parallel to the H_2O/THF line in *Figure 1*, keeping the polymer–water ratio constant. Due to the rapid movement of the particles by the adsorbed heat on the evaporation of THF, taking the photographs was difficult at least up to 30 s. Therefore, microscopic observations observed by changing time were sketched and are represented in *Figure 2*. The magnification here was 1000 times. About 20 s after the solution was dropped, particles with diameter of about 0.2 μm began to appear. The particles became larger, probably due to the coarsening in the spinodal decomposition, until 40 s after the solution was dropped. The violent movement of the particles mentioned above ceased at this stage. The photomicrographs taken at this stage are shown in *Figure 3*. At 1 min after dropping of the solution, the size of the particles became uniform with diameter of about 10 μm. At 2 min after the solution

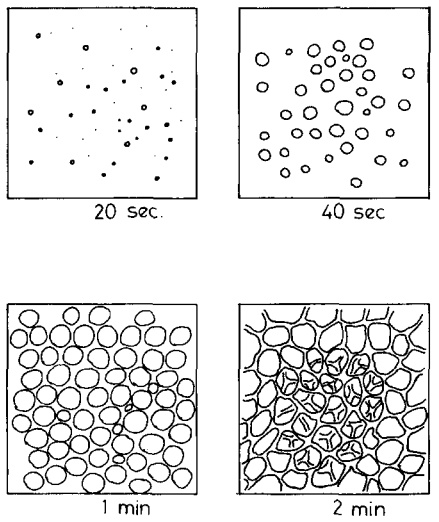

Figure 2 The sketch of the observation of the phase separation in the system, PVC/THF/water: 6.9/83.9/9.2 (wt%), under a microscope. The evaporation time is shown

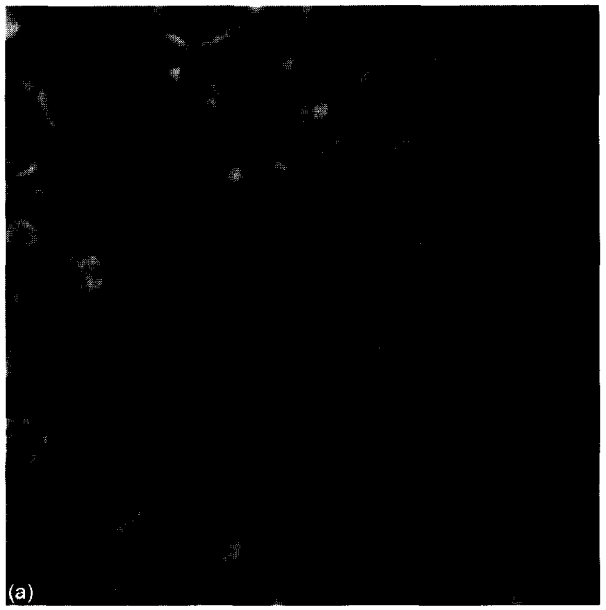

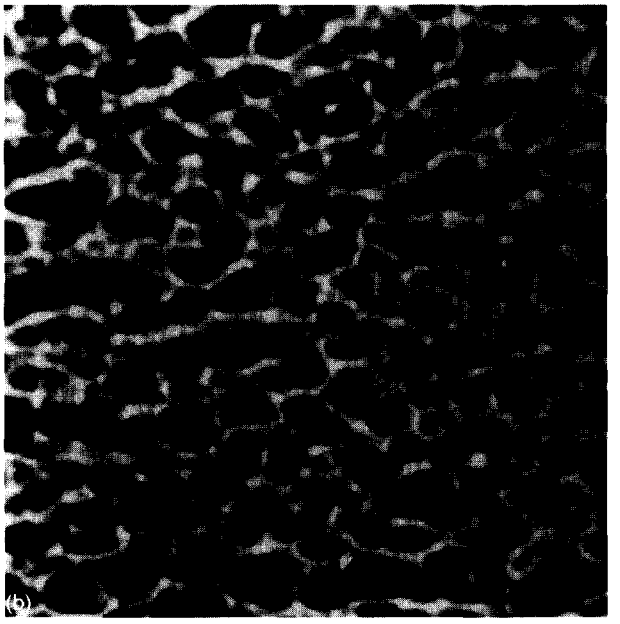

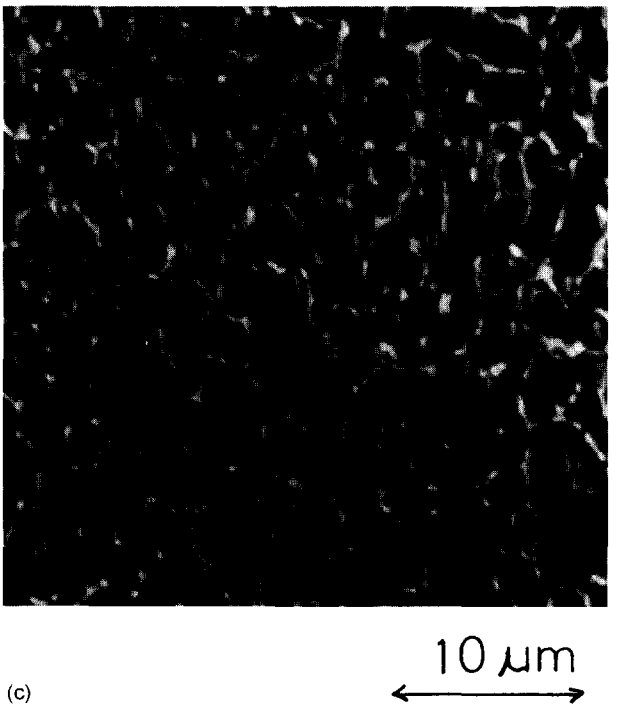

Figure 3 Optical micrographs taken at (a) 40 s, (b) 1 min and (c) 2 min, respectively, after the evaporation of THF started from the system, PVC/THF/water: 6.9/83.9/9.2 (wt%). (a) At 40 s

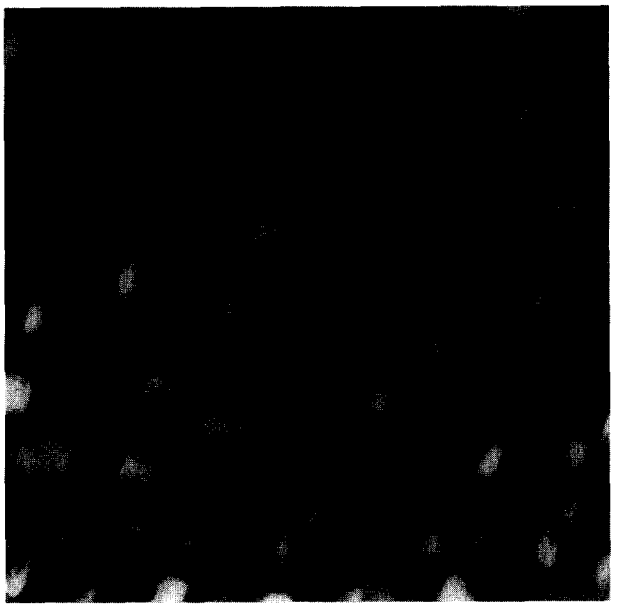

(a)

(b)

Figure 4 Optical micrographs showing the growth of the particles when the evaporation of THF stopped at the stage, 40 s after the dropping of the solution, PVC/THF/water: 6.9/83.9/9.2 (wt%)

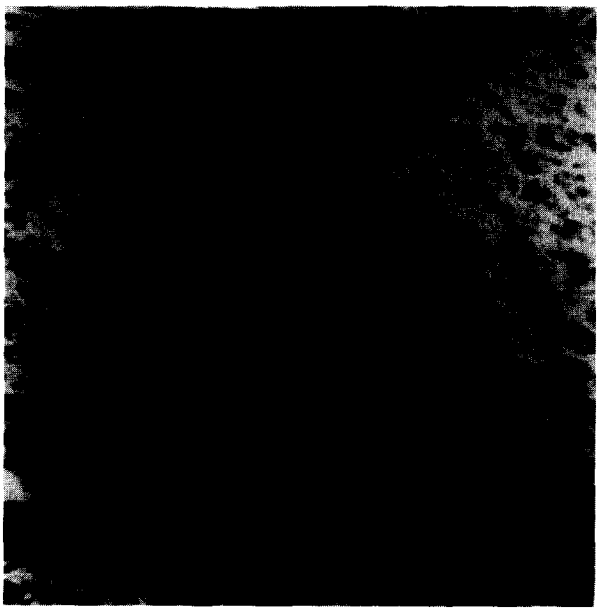

Figure 5 A scanning electron micrograph of the cross-section of the membrane obtained from the system, PVC/THS/water: 6.9/83.9/9.2 (wt%) by the evaporation of THF

Table 1 Compositions of the polymer-lean phase and the polymer-rich phase in the phase separation of the system, PVC/THF/water at 20°C

		Composition (wt%)		
Phase ratio	Phase	PVC	THF	H_2O
0.274	O	7.00	82.7	10.3
	L	3.26	83.5	13.3
	R	7.67 (7.85)	82.9 (82.5)	9.39 (9.63)
0.957	O	4.70	84.0	11.3
	L	2.45	84.5	13.0
	R	6.83 (6.74)	86.8 (83.5)	6.39 (9.71)
5.00	O	2.40	84.9	12.7
	L	1.20	85.1	13.7
	R	(7.90)	–(84.0)	–(8.10)
14.0	O	1.20	85.4	13.4
	L	0.73	85.6	13.7
	R	–(7.31)	–(90.2)	–(2.94)

O, original (before phase separation); L, polymer-lean phase; R, polymer-rich phase. The values in parentheses are calculated from the total mass-balances

was dropped, pores with a closed compact state were formed.

From the phase diagram (*Figure 1*), it is evident that the particles mentioned above consist of the polymer-lean phase. This could be easily confirmed by changing the position of the focus of the microscope up and down, due to the difference in the refractive index of the two phases. When the evaporation of the solvent was restricted by putting the cover glass onto the solution, the particles continue to grow and their number decreases, as shown in *Figure 4* [i.e., from (a) to (b)]. Therefore, during the formation of such membranes, the competition between the nucleation and the growth of particles should occur and thus influences the pore size distribution of the resulting membrane.

Figure 5 shows a SEM picture of the cross-section of the membranes obtained through the above procedure. Although this is the micrograph of the cross-section of the membrane, the features here are quite similar to those of *Figures 3b* and *c*. Due to the closed packed state that arose during the process of the formation of the membrane, rather uncircular pores with a narrow pore size distribution resulted. This may support the spinodal decomposition and the coarsening mechanism, rather than that of the nucleation and growth mechanism.

Table 1 shows the result of the phase separation experiment at 20°C. The values in the parentheses were calculated by considering the total mass balances. In the upper two cases in the table, the measured values for the polymer-rich phase roughly coincide with those

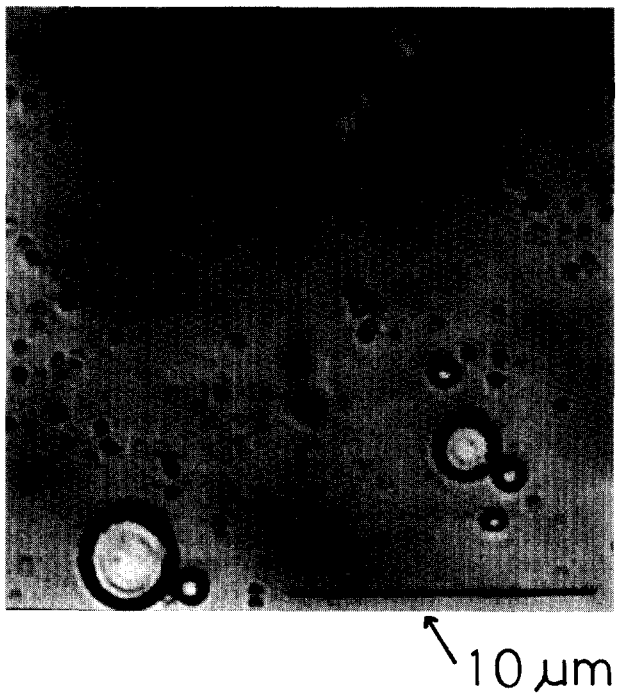

Figure 6 An optical micrograph of polymer particles obtained on casting the solution of the composition, B in *Figure 1*

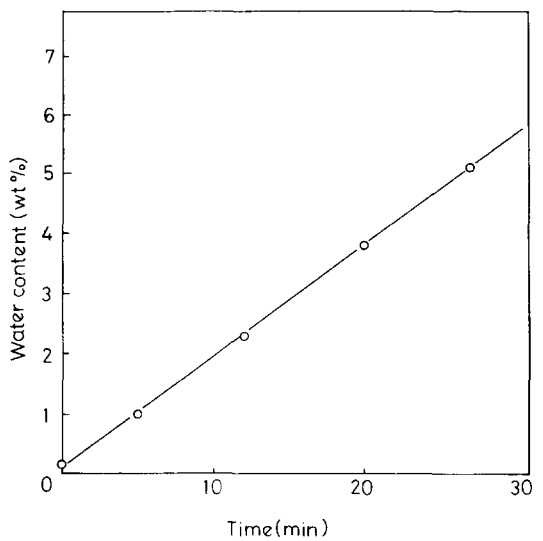

Figure 7 The absorption of water by DMF measured as a function of time at 33.5°C under 65% RH

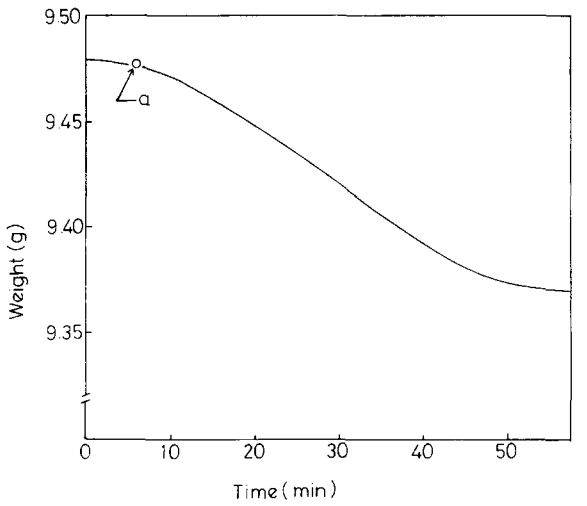

Figure 8 The change in the weight of a 11.1% PVC solution in DMF with time at 32°C under 65% RH. The point a shows the cloud point

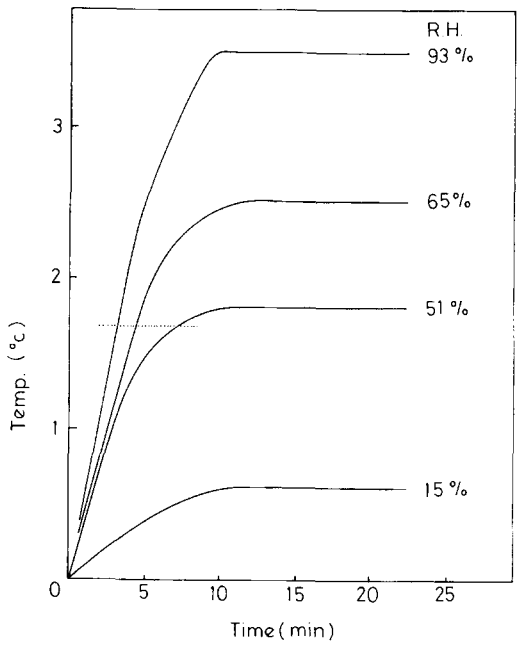

Figure 9 The rise in the temperature of a 9.5% PVC solution in DMF as a function of time at 33.5°C under various RHs. The dotted line indicates the cloud point

calculated. Since the polymer-rich phase in the lower two cases of the table was too viscous to put into the thin glass tube used for the gas chromatography, only the calculated values were shown for the polymer-rich phase. The polymer concentration at the critical point in this system was *ca.* 3.5% (*Figure 1*). The polymer composition was less in the polymer-lean phase and higher in the polymer-rich phase than the original composition, when the phase ratio, i.e. the volume ratio of the polymer-lean phase to the polymer-rich phase, was less than unity. Naturally, the opposite applies to the case where the phase ratio exceeds unity. Of course, in the case when the phase ratio is less than unity (i.e. for the original higher composition of polymer), the polymer-lean phase should be suspended in the polymer-rich phase when the system was disturbed, whereas the opposite holds when the phase ratio is greater than unity. Although these data can be predicted qualitatively by the theory, the results may afford some information on, for instance, how the non-solvent should move from one phase to another surrounding phases.

The formation of the membrane was also tried by casting from the composition of solution corresponding to the point B in *Figure 1* and evaporating THF. This should start the phase separation where the polymer-rich phase is surrounded by the polymer-lean phase. *Figure 6* shows the polymer particles appeared in the system after drying. Some signs of the agglomeration of the particles are seen, but the agglomerate with continuous structure could not be obtained. It may be postulated from the spherical nature of the particles, however, that the

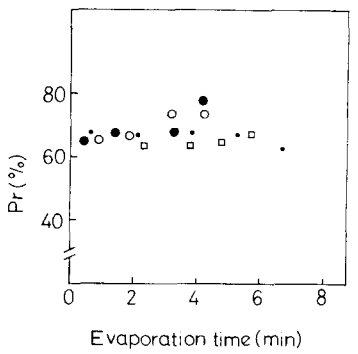

Figure 10 The porosity, P_r, of the membrane plotted against the evaporation time for the various compositions of casting solutions. (●), PVC/DMF/$CaCl_2 \cdot 2H_2O$/MeOH = 9.2/82.5/1.4/6.9; (○), PVC/DMF/$CaCl_2 \cdot 2H_2O$/MeOH = 9.2/83.1/0.8/6,9; (□), PVC/DMF/MeOH = 9.7/87.4/2.9; (▪), PVC/DMF = 11.1/88.9

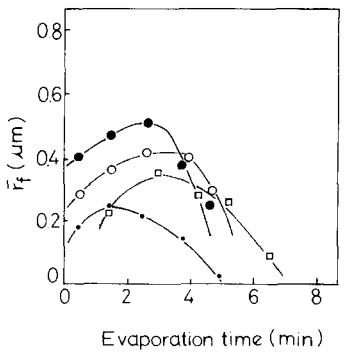

Figure 11 The mean pore radius, $\bar{r}_f$, of the membrane plotted against the evaporation time for the various compositions of casting solution. (●), PVC/DMF/$CaCl_2 \cdot 2H_2O$/MeOH = 9.2/82.5/1.4/6.9; (○), PVC/DMF/$CaCl_2 \cdot 2H_2O$/MeOH = 9.2/83.1/0.8/6.9; (□), PVC/DMF/MeOH = 9.7/87.4/2.9; (▪), PVC/DMF = 11.1/88.9

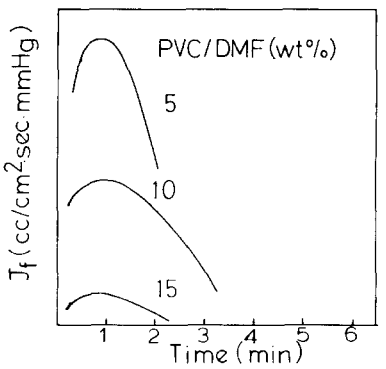

Figure 12 The flux, J_f, of methanol through the membrane cast from the different concentrations of PVC solutions in DMF. The PVC concentration (PVC/DMF wt%) is indicated on each curve

nucleation and growth mechanism of the polymer-rich phase in the polymer-lean phase holds in this case.

PVC/DMF/water system

When the solution of PVC in DMF was cast and dried, porous membrane appeared with the diameter ranging from 0.1 to 4 μm. It became apparent that this was due to the absorption of water in air by DMF during the evaporation of DMF. *Figure 7* shows the water content in DMF plotted against time at 33.5°C under RH of 65%. It is apparent that DMF absorbs water linearly with time.

Figure 8 shows the change in weight of a 11.2% PVC solution in DMF with time at 32°C under 65% RH. The decrease in weight observed indicates that the amount of DMF evaporated from polymer solution exceeds the absorbed amount of water in DMF. The point a shown in the curve indicates the cloud point where the phase separation started. The curve became steeper from the point a and levelled off at 45 min. This may reflect changes that occurred in the solution or gel state.

Figure 9 shows the temperature rise that occurred during the formation of the membrane cast from a 9.52% PVC solution in DMF as a function of the evaporation time at 33.5°C under the various RHs. The higher the RH, the steeper the slope of the curve, and all the curves level off beyond about 10 min. The rise in temperature is considered to be due to the heat of mixing of water and DMF. The more rapid rise in temperature under higher humidity observed may reflect higher rate of dissolution of water into DMF, if the rate of evaporation of DMF is independent of RH. In fact, the rate of the rise in temperature was proportional to RH, which indicates that Henry's law is obeyed, though not shown here. The dotted line drawn in *Figure 9* indicates the points where the membrane became opaque. This shows that provided the temperature rise is proportional to the water content in the membrane, the water content, absorbed by the membranes until they became turbid due to the phase separation is constant. The levelling off of the curves is considered to be due to the balance between the heat evolved by the absorption of water and the loss of the heat by the evaporation of DMF attained.

The above results show that the conditions of the phase separation, and accordingly, the pore formation in the membrane in this system is rather complicated so that the evaporation of DMF (i.e. the increase in the polymer composition) and the absorption of water cooperatively enhance the phase separation in the membrane and moreover, the temperature of the system changes during the phase separation. It seems that the effect of the water content prevails over the other two factors just-mentioned. Before the cloud point, where the water content in the solution is constant as a function of RH of the atmosphere, as shown previously, the solution suddenly contacts with water. On the other hand, after the cloud point, where the phase separation occurred in the solution, the situation becomes similar to the case of the PVC/THF/water system discussed previously, in a sense that the initial instantaneous phase separation occurred in the solution of the PVC/solvent/nonsolvent system. In fact, the observation under a microscope showed similar behaviour to that shown in *Figures 2* and *3* for the case of the PVC/THF/water system. Although the phase diagram was not determined precisely as in the PVC/THF/water system, the polymer composition at the critical point was estimated to be less than 5%. Therefore, in all the cases studied, the polymer-lean phase should be dispersed in the polymer-rich phase. It is thus postulated that the spinodal decomposition and coarsening should occur also in this system.

In the case where the membrane was formed prior to the cloud point, the phase separation occurring at the interface between the membrane and water should be so fast that the spinodal decomposition and the coarsening will make a rather compact and continuous skin layer, and an asymmetric membrane will be formed. Though

not shown, the scanning electron micrographs of such membranes showed that asymmetric membranes were formed. The membrane obtained by evaporating DMF for 1 min from a 15.7% PVC solution and quenched in water showed a pore density of $3.3 \times 10^5 cm^{-2}$ on the surface, as calculated from many micrographs. Using $\bar{r}_e$ obtained as 0.12 μm, the porosity of the surface was calculated to be only 1.0%, whereas the overall porosity calculated from the weight and the thickness of the membrane was 69%.

In fact, all the membranes studied were asymmetric. In *Figure 10*, the porosity, P_r, of the membrane was plotted against the evaporation time for the various compositions of casting solutions. In all the cases studied, the porosity measured was nearly constant ranging from 60% to 70%, independent of the evaporation time and accordingly, of the pore size. This, of course, indicates that all the membranes formed are asymmetric, so that a much larger amount of the supporting layer governs the porosity of the membrane. As well known, the permeability of such an asymmetric membrane was governed by the surface skin layer.

Figure 11 shows the average pore size, $\bar{r}_f$, calculated from the flux of methanol through the membrane by using equation (3), as a function of the evaporation time for the membranes cast from the various compositions of solutions. Since the permeation of methanol through the membrane should be determined by the thin skin layer as mentioned above, $\bar{r}_f$, determined by equation (3) using the thickness, d, and the porosity, P_r, of the total membrane may be meaningless[16]. Since the thickness and porosity of the membranes observed were nearly constant, namely, d, being in the range of 90–110 μm and P_r, in the range of 60–70% as shown in *Figure 11*, however, the relative magnitude of $\bar{r}_f$ at least can be discussed. Especially, the thickness of the skin layer as observed by a scanning electron microscope was nearly constant as usually observed on asymmetric membranes[16]. Therefore, *Figure 11* may be considered to reflect directly the relative magnitude of the flux of methanol through the membrane. However, the order of the magnitude of $\bar{r}_f$ coincided well with that of $\bar{r}_e$ obtained from the electron micrographs, since the skin layer was *ca.* 100 times smaller than the whole membrane and the porosity of the skin layer as observed by electron microscope was *ca.* 70–100 times smaller than that of the overall membrane [cf. equation (3)]. In fact, the relative mean pore size, $\bar{r}_f$, nearly corresponded to that of $\bar{r}_e$.

All the curves in *Figure 11* show a maximum, at the time corresponding to the onset of the phase separation in each system. Before the cloud point, the mean pore radius (accordingly, the flux of methanol) is considered to increase due to the decrease in the supersaturation at the interface between PVC solution and water as the evaporation proceeds. After the cloud point, phase separation proceeds in the membrane successively from the top surface to the bottom with the evaporation time, and is finally followed by rapid quenching, when the membrane is immersed in water. The decrease in the mean pore radius at this stage may be due to the shrinkage of the membrane by the evaporation of the solvents during the processes mentioned above, including the drying of the membrane.

In *Figure 12* is shown the flux of methanol through the membrane plotted against the evaporation time, changing the original PVC concentration in the casting solution in DMF. It can be easily understood that the membrane with lower porosity and lower pore radii in the skin layer is formed from the solution of higher polymer concentration (see *Table 1*), showing the lower flux through the membrane. The steeper decrease in the flux after the cloud point for the lower polymer concentration supports the above-mentioned view that the mean pore radius decreases by the shrinkage of the membrane.

The results of the flux of methanol through the membranes measured by adding methanol into the original solution showed that the flux vs the evaporation time curves moved to longer times, meaning that the cloud point was delayed by the addition of methanol, which simply indicated that methanol weakened the precipitation power of water. Finally, as shown in *Figure 11*, the mean pore radius increased by the addition of $CaCl_2$ and the evaporation time at the cloud point was delayed as in the case of the addition of methanol. It is known[2,14,17] that the addition of inorganic salts stabilizes the system where the phase separation is occurring, which makes the formation of the uniform membranes easier.

REFERENCES

1 Loeb, S. and Sourirajan, S. UCLA Dept. of Chem. Eng. Report 1958, No. 58-26
2 Koros, W. J. and Pinnau, I. 'Polymeric Gas Separation Membranes' (Eds D. R. Paul and Y. P. Yampol'skii), CRC Press, 1994, p. 209
3 Broens, L., Koehnen, D. M. and Smolders, C. A. *Desalination* 1977, **22,** 205
4 Koehnen, D. M., Mulder, M. H. V. and Smolders, C. A. *J. Appl. Polym. Sci.* 1977, **21,** 199
5 Smolders, C. A. 'Ultrafiltration and Applications' (Ed. I. Cooper), Plenum Press New York, 1980, p. 161
6 Perepechkin, L. P. *Russ. Chem. Rev.* 1988, **57,** 959
7 Burghardt, W. R., Yilmaz, L. and McHugh, A. *J. Polymer* 1987, **28,** 2085
8 Cohen, C., Tanny, G. B. and Prager, S. *J. Polym. Sci., Polym. Phys. Ed.* 1979, **17,** 449
9 Cahn, J. W. *J. Chem. Phys.* 1965, **42,** 93
10 Nishi, T., Wang, T. T. and Kwei, T. K. *Macromolecules* 1975, **8,** 227
11 Tsai, F. J. and Torkelson, J. M. *Macromolecules* 1988, **21,** 1026
12 Kamide, K. and Manabe, S. ACS Symposium Series No. 269 (Ed. D. R. Lloyd), 1982, p. 197
13 Cleland, R. L. and Stockmayer, W. H. *J. Polym. Sci.* 1955, **17,** 473
14 Kamide, K., Manabe, S., Matsui, T., Sakamoto, T. and Kajita, S. *Kôbunshi Ronbunshû Japan* 1977, **34,** 205
15 Islam, M. A. and Stoicheva, R. N. *J. Membrane Sci.* 1994, **92,** 209
16 Kawai, T., Lee, Y. M. and Fujita, H. *Korea Polym. J.* in press
17 Otto, E. and Spurlin, H. M. 'Cellulose and Cellulose Derivatives', 2nd Edn, Vol. 5, Part 3, Interscience, New York, 1955